JOURNAL OF THERMOPHYSICS AND HEAT TRANSFER
Vol. 16, No. 1, January–March 2002

Technical Notes

TECHNICAL NOTES are short manuscripts describing new developments or important results of a preliminary nature. These Notes cannot exceed six manuscript pages and three figures; a page of text may be substituted for a figure and vice versa. After informal review by the editors, they may be published within a few months of the date of receipt. Style requirements are the same as for regular contributions (see inside back cover).

Rectangular Jet Impingement Heat Transfer on a Vehicle Windshield

Subrata Roy,* Karim Nasr,† and Paresh Patel‡
Kettering University, Flint, Michigan 48503
and
Bashar AbdulNour§
Ford Motor Company, Dearborn, Michigan 48120

Introduction

THE flow of an impinging air jet on an inclined surface addresses a number of practical applications including defogging and deicing of a vehicle's windshield, vertical/standard takeoff and landing engineering, and film cooling of turbine blades. The specific application of interest is air issuing from the defroster's nozzles of a vehicle and impinging on the glass windshield. Various factors can be examined for optimizing the flow performance for defrosting ice on the outside surface or clearing fog on the inside surface. The nozzle outlet must be capable of generating an airflow that disperses over the entire inner surface of the windshield.

The interaction of multiple cool air jets with hot inclined wall generates complex flowfields that have been extensively investigated in the literature.[1–4] A number of investigators have tackled the specific problem of air issuing from the defroster's nozzles and impinging on the inclined surface of a vehicle's windshield.[4–7] The purpose of such investigations is to enhance the defroster's performance in providing clear areas free of frost or fog. A recent survey of relevant investigations[8] points to the heat transfer coefficient being the primary controlling parameter influencing heat transfer between the fluid and the solid surface.

In this Note the fluid-thermal characteristics of a pair of impinging rectangular jets on a windshield are identified. Experimental measurements of local surface temperatures are used to yield local heat-transfer coefficient for an imposed heat flux. Corresponding three-dimensional numerical simulation is performed using a commercial finite volume code for obtaining detailed temperature and flow distributions. The solution is validated with experimental data, and the predicted local and average heat transfer coefficients on the internal surface of an inclined windshield are compared.

Received 6 February 2001; revision received 20 August 2001; accepted for publication 14 September 2001.

*Assistant Professor, Mechanical Engineering Department; sroy@kettering.edu. Associate Fellow AIAA.
†Associate Professor, Mechanical Engineering Department; knasr@kettering.edu.
‡Graduate Student, Mechanical Engineering Department; ppatel@kettering. edu. Student Member AIAA.
§Technology Development Department; babdulno@ford.com.

Experimental Setup

An experimental apparatus consisting of the HVAC module of a car and a windshield was assembled. A thin heating pad, 0.3048 m wide and 0.4572 m long, was attached centrally to the outer surface of the windshield providing constant surface heat flux in that region. Air is forced onto the inclined windshield, via the blower of the HVAC module, impinges and hugs the large surface of the windshield, and disperses into the laboratory environment. The main base of the test stand is intentionally kept open for unrestricted placement, adjustment, and accessibility of the HVAC module components. To allow for the possible adjustment of the windshield's angle between the windshield and dashpad, two pillars, made of 3.81-cm perforated steel angle, were affixed to the stand.

A representative windshield angle of a passenger vehicle was chosen as 39 deg, which is the angle used for the experiments. A pair of 12.7-cm bolts was placed in the appropriate pillar holes to support the windshield at the desired angle. To power the blower of the HVAC module, a 12V ac-dc power converter was chosen, wired into the blower unit and tested. In the actual application the air is heated via a heater core and impinges on the windshield. In the current experiment unheated room air impinges on a heated windshield. The windshield is heated partially on its outer surface via a thermal heating pad, as mentioned earlier. The heater is capable of producing approximately 540 W. The back surface of the heating pad is insulated via a polystyrene insulation layer of known R value.

A variable resistor potentiometer was used in conjunction with two digital multimeters (DMM) for the purpose of controlling the heat flux. One DMM was used to measure the voltage while the other yielded the current. Of course, the heating pad wattage (input) is the product of volts and amps. The convected heat by the flowing air is computed by $Q_{\text{conv}} = Q_{\text{input}} - Q_{\text{loss}} - Q_{\text{rad}}$, where $Q_{\text{loss}} = \Delta TA/R$ is the rate of heat transfer, in watts, off the back surface of the heater. This heat loss was quantified based on the temperature difference ΔT of the back surface of the heater and the outer surface of the insulation pad. Q_{rad} is the radiative heat transfer exchanged between the inner surface of the windshield and the surroundings, $Q_{\text{rad}} = \varepsilon\sigma A(T_s^4 - T_{\text{surr}}^4)$.

Numerical Model

Figure 1 is a schematic of the vehicle windshield and its associated air volume. The air jet, at temperature T_j, issues at an angle ϕ through two rectangular openings and impinges upon the glass windshield of thickness t. The windshield is inclined at an angle α and has a heating pad that is centrally placed on the external surface of the windshield. The heating pad introduces a constant heat flux into the heated area. All necessary dimensions are given in the figure. The mean plug flow velocity in the injection pipe is V.

The system of equations for steady, turbulent, buoyancy-driven, incompressible jet flows, including the k–ε model, has been studied in detail in the literature.[9] For state variable $\boldsymbol{q} = [1\ u\ v\ w\ k\ \varepsilon\ T]^T$, the transformed equations for the intrinsic coordinate system ξ_i can be written as[10]

$$\frac{\partial \boldsymbol{f}^{\xi_i}}{\partial \xi_i} = \frac{\partial}{\partial \xi_i}\left(\boldsymbol{f}_v^{\xi_i} + \hat{\boldsymbol{f}}_v^{\xi_i}\right) + \boldsymbol{S} \tag{1}$$

where source term $\boldsymbol{S}$ includes the Boussinesque approximation for the momentum equation, $\boldsymbol{f}^{\xi_i}$ is the convective flux vector, and $\boldsymbol{f}_v^{\xi_i}$ and $\hat{\boldsymbol{f}}_v^{\xi_i}$ are the diffusive flux vectors.

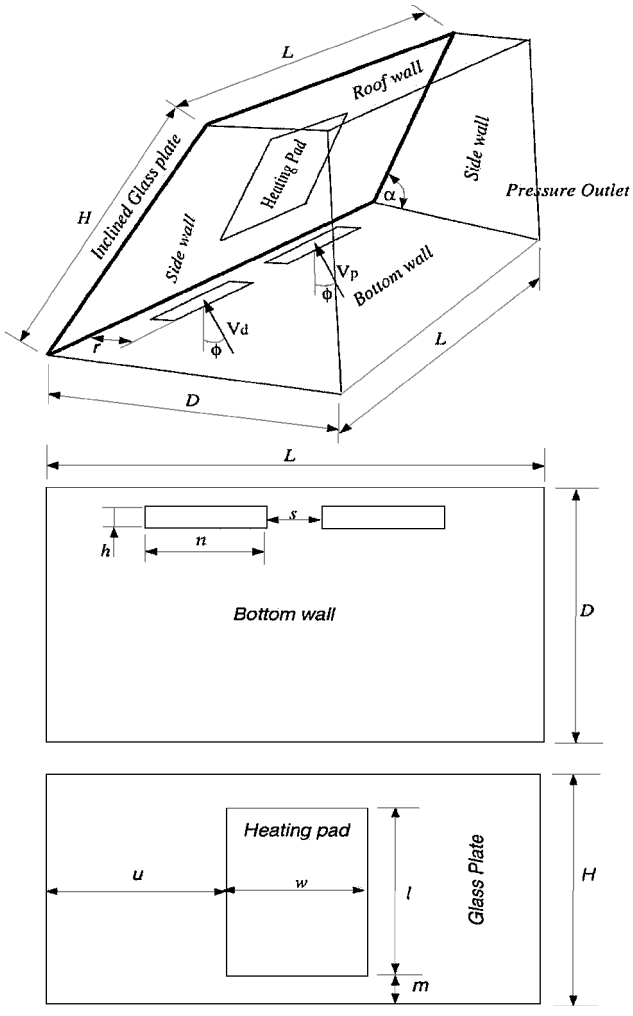

Fig. 1 Schematic of the simulation domain.

In this work we utilized the renormalization group based k–ε model.[11] This model introduces two equations, one for the turbulent kinetic energy k and the other for its dissipation rate ε. These equations are included in the set of the transformed Eq. (1). The effect of this model is to introduce an additional viscosity, called turbulent viscosity. The turbulent viscosity is not a fluid property, but rather a property of the flowfield. Its value is added to the molecular viscosity and yields an effective viscosity, which is used in the computational model. The k and ε at the inlet are calculated from the following expressions: $k_{\text{in}} = 1.5(T_u u)^2$ and $\varepsilon_{\text{in}} = k_{\text{in}}^{1.5}/L_\varepsilon$, where T_u is the turbulence level and L_ε is a characteristic length of the domain.

Equations (1) and (2) constitute a system of nonlinear algebraic equations. The system is linearized by relaxation. A streamline upwinding technique[12] is employed for stabilizing numerical iterations. The pressure corrections are used to correct the pressure and the velocities.[13] This predictor–corrector procedure constitutes one iteration. The solution is declared convergent when the maximum residual for each of the state variable becomes smaller than a convergence criterion of 10^{-4}.

Results and Discussion

Experimental Results

The experiment was performed at a fixed blower setting and a heating pad power value of $Q_{\text{input}} = 67.5$ W. For this power input the heat flux $Q_{\text{input}}/A = 484.4$ W/m^2. The heat flux loss through the polystyrene insulation pad was calculated to be $Q_{\text{loss}}/A = 29.43$ W/m^2, and the net radiative flux off the inner surface of the windshield was computed to be $Q_{\text{rad}}/A = 87$ W/m^2.

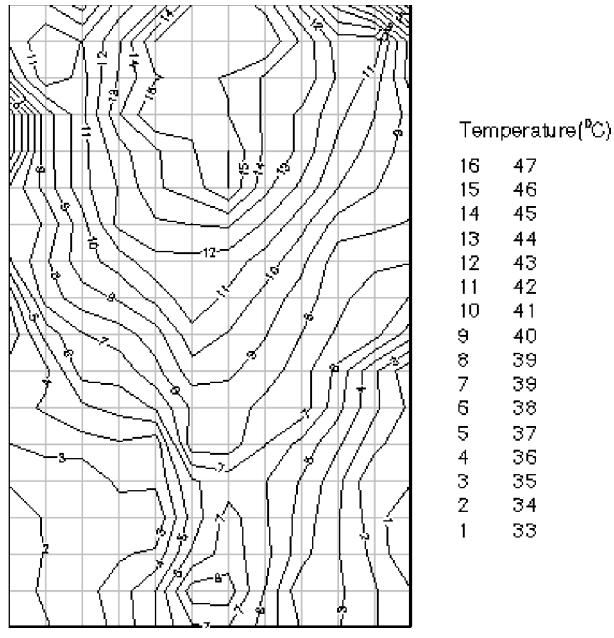

Fig. 2 Experimentally based temperature contours on the heated area of the windshield.

Therefore, the convective flux to the flowing air was found to be $Q_{\text{conv}}/A = 368$ W/m^2. Newton's law of cooling was employed to evaluate the local heat transfer coefficients:

$$h = \frac{Q_{\text{conv}}}{A(T_S - T_{\text{in}})} \tag{2}$$

The incoming air temperature was recorded as $T_{\text{in}} = 25.5$°C by placing a type T thermocouple at the outlet of the blower ductwork, that is, at the defroster nozzle's exit plane. The local surface temperature of the windshield was measured by mapping the heated area of the windshield with 100 strips of temperature-sensitive liquid crystals.

A grid was formed on the windshield under the entire surface of the heating pad by drawing horizontal and vertical lines with a 2.54-cm spacing. This grid was used to record the location of the point at which the inner surface temperatures were detected. Embedded in the plastic were pieces of liquid crystal temperature sensing strips. As a result, a map of local surface temperatures was generated. Figure 2 displays an Excel-generated map (contours) of temperature values. The local surface temperature gives a local heat-transfer coefficient via Eq. (2). A grid is constructed of 12 cells laterally and 18 cells longitudinally on the inner side of windshield as shown in Fig. 2.

Errors in computing the value of the heat transfer coefficient could result from the measurement of the voltage, the current, the heat losses, the surface area, the surface temperature, and the incoming jet air temperature. Performing uncertainty analysis using the root-sum-square method[14] and computing individual relative uncertainties yielded a 5.1% relative uncertainty in the value for the heat-transfer coefficient. The average heat transfer coefficient over the heated area of the windshield was then computed as $\bar{h} = 1/A \int h \, dA$ and found to be 29.4 W/m^2 K. The numerical simulation discussed in the next section compares local temperatures as well as experimental and numerical heat transfer coefficients.

Numerical Predictions

The schematic of the simulation volume is shown in Fig 1. A vertical ($\phi = 0$ deg) air jet at uniform temperature $T_j = 25.5$°C $= 298.5$ K is impinging upon the windshield of thickness $t = 0.006$ m inclined an angle $\alpha = 39$ deg. The injection ducts are rectangular slots with $n = 0.241$ m and $h = 0.019$ m. The distance between the slot centers $s = 0.127$ m. The geometric dimensions of the windshield and its layout match exactly those set up experimentally. In Fig. 1 for

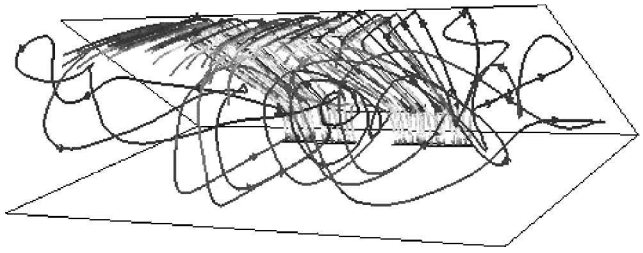

Fig. 3 Particle tracks showing full three dimensionality of the flowfield.

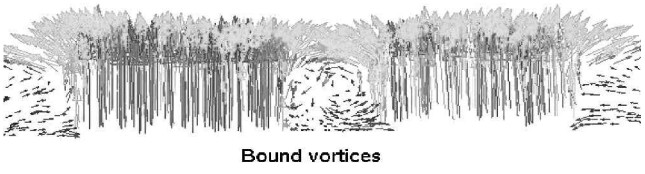

Fig. 4 Velocity vector distribution on the plane cutting through the defrosters shows bound vortices.

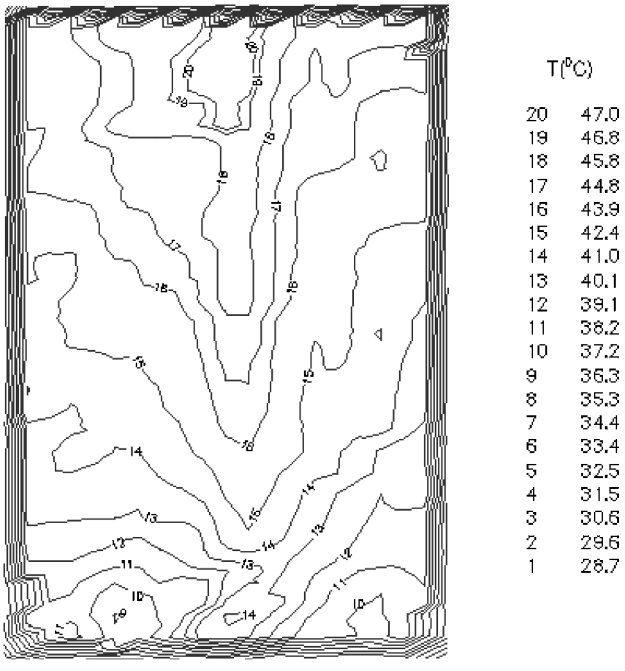

Fig. 5 Temperature distribution on the inside surface of the windshield across the heating pad.

the bottom, side, and top surfaces of the control volume and on the inside of the windshield, typical wall boundary conditions are used, that is, the no-slip condition for the velocities and wall functions for k and ε. The axial velocity profiles V_d and V_p are prescribed over the openings; $k = k_{\text{in}}$ and $\varepsilon = \varepsilon_{\text{in}}$ are prescribed at the inlets by choosing an appropriate T_u. Finally, a constant heat flux is applied through the heating pad. The downstream conditions are zero gradients for all state variables.

The average velocity at the inlet and the imposed heat-flux values were determined experimentally and used for the numerical investigation. The mean flow velocity in the injection pipes are specified as uniform for both driver side V_d and passenger side V_p, and $V_d = V_p = 8$ m/s. The heating pad for the numerical simulation is bounded by $l = 0.457$ m in the longitudinal direction and $w = 0.305$ m in the lateral direction. A uniform heat flux of 368 W/m^2 is applied on this area of the windshield. The inlet section is located at $r = 0.134$ m and the exit at $D = 0.896$ m. The other dimensions as shown in Fig. 2 are $L = 1.447$ m, $H = 0.719$ m, $u = 0.569$ m, and $m = 0.131$ m. Despite the symmetry of the geometric configuration, the entire domain is considered for analysis. The density, specific heat, and thermal conductivity of windshield glass are 2500 kg/m^3, 750 J/kg-K, and 1.4 W/m-K, respectively.

A computational mesh of 127,156 tetrahedral finite volumes was created using commercial mesh generation software. The maximum distance between the wall and the first grid point varies between y^+ of 2.5 for the windshield to y^+ of 15 for the coarsest mesh. The turbulence level was chosen equal to 10% (i.e., $T_u = 0.1$). Factors such as mesh density, cell geometry, turbulence model including the choice of turbulence level, degree of approximation of the describing equations, error criterion for convergence, and numerical control parameters, can severely impact the speed and accuracy of the numerical solution.[10]

The three-dimensional Navier–Stokes Eqs. (1) are solved for this fluid-thermal system using a finite volume commercial code. The computational fluid dynamics (CFD) solutions are documented in Figs. 3–6. Figure 3 is a three-dimensional view of the airflow characteristics inside the computational domain showing outlines of the inclined windshield, the heating pad, the inlets (defroster's nozzles), and the side walls. Tracking 12 particles released from each inlet shows complex three-dimensional pathlines of fluid flow.

Velocity vectors plotted on two-dimensional cross section of the simulation volume on a vertical plane passing through the center of both the jets captures the vortical flow patterns in Fig. 4, exhibiting recirculation and flow issuing regions. The impinging fluid forms a bound vortex structure on this plane between the jets bending the fluid downward. The jets coming out of the defroster openings appear to the flow deflected by the windshield as solid. A sharp velocity and temperature gradient is formed upstream of the jet while a wake region develops downstream of the jet. In the latter, a pair of bound vortices per jet is formed, which bends the jet both downward and upward, producing the well-known kidney shape in streamline contours.

The jet impingement process tremendously affects the temperature distribution on the windshield. The air attached to the

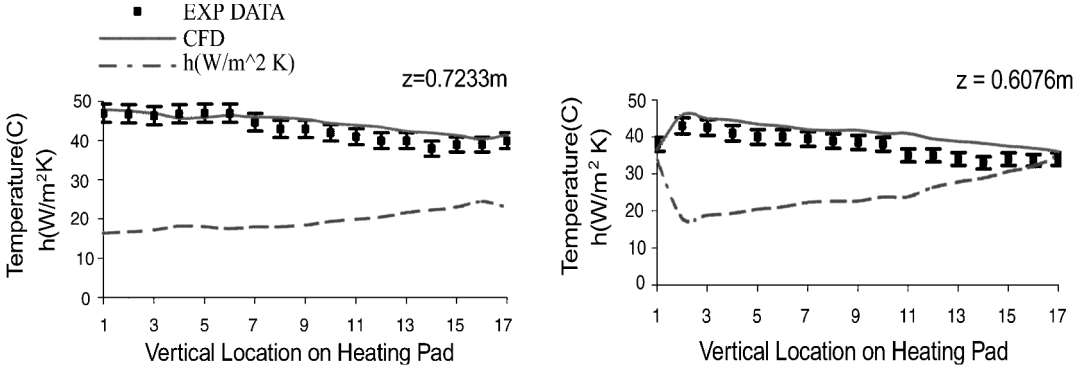

Fig. 6 Validation of CFD results with experimental data at different locations on the heating pad.

windshield is coming off the plane at the top of the plot. This complex three-dimensional nature of the fluid flow has significant influence on the heat transfer process between the jet and the inclined surface as well as inside the simulation volume. Higher velocity near the wall causes a local cooling effect as a result of higher convective heat transfer. The temperature contours on the inside surface of the windshield under the heated area in Fig. 5 show an overall comparison between the experimental data (Fig. 2) and CFD prediction of thermal patterns.

The predicted temperature distribution on the inside of the heating pad should also be compared with the experimental data on a point-by-point basis. A detail comparison of predicted and experimental temperature distribution done on 17 points at each of the two constant z lines along the inside of the windshield under the heating pad (Fig. 6). The line $z = 0.7233$ m identifies the central location between the issuing jets, while $z = 0.6076$ m passes through the passenger side jet. Documented results validate the numerical prediction within 1–3°C of the measured temperature values. Corresponding heat transfer coefficients h, computed via Eq. (2), are also plotted in the same figure. The average heat transfer coefficient from the predicted numerical results is $\bar{h} = 25.68$ W/m^2 K.

Conclusions

This Note addressed numerical and experimental studies of a pair of rectangular air jets impinging on an inclined surface. Experimental measurements of surface temperatures, using liquid crystals, yielded a map of local heat transfer coefficients between the surface and the incoming jet for an imposed heat flux. Corresponding three-dimensional numerical simulation has been performed using a finite volume algorithm for obtaining detailed temperature and flow distributions. The numerical simulation correlated reasonably well with the experimental results and further explained the flow characteristics and thermal patterns. A detail comparison of 34 locations under the heating pad validated the numerical predictions within 1–3°C of the measured temperature values. Further investigation should aim for the defogging/defrosting analysis in the flow.

References

[1]Polat, S., Huang, B., Mujumdar, A. S., and Douglas, W. J. M., "Numerical Flow and Heat Transfer Under Impinging Jets: A Review," *Annual Review of Numerical Fluid Mechanics and Heat Transfer*, Vol. 2, 1989, pp. 157–197.

[2]Martin, H., "Heat and Mass Transfer Between Impinging Gas Jets and Solid Surfaces," *Advances in Heat Transfer*, Vol. 13, Academic Press, New York, 1977, pp. 1–60.

[3]Downs, S. J., and James, E. H., "Jet Impingement Heat Transfer—A Literature Survey," American Society of Mechanical Engineers, Paper 87-HT-35, Oct. 1987.

[4]Viskanta, R., "Heat Transfer to Impinging Isothermal Gas and Flame Jets," *Experimental Thermal and Fluid Science*, Vol. 6, No. 2, 1993, pp. 111–134.

[5]Carignano, M., and Pippione, E., "Optimization of Wind-Screen Defrosting for Industrial Vehicles via Computer Assisted Thermographic Analysis," FIJITA Paper 905237, 1990.

[6]Andreone, L., Burzio, G., Damiani, S., and Romitelli, G., "Automatic Measurement of Defrosting/Defogging Process," ATA Paper 92A272, 1992.

[7]Willenborg, K., Foss, J. F., AbdulNour, R. S., McGrath, J. J., and AbdulNour, B. S., "A Model Defroster Flow," *Proceedings of the Eleventh Symposium on Turbulent Shear Flows*, Vol. 2, edited by G. Binder, Centre National de la Recherche, Grenoble, France, 1997, pp. 15.25–15.30.

[8]Nasr, K. J., and AbdulNour, B. S., "Defrosting of Automotive Windshields: Progress and Challenges," *International Journal of Vehicle Design*, Vol. 23. Nos. 3–4, 2000, pp. 360–375.

[9]Johari, H., Pacheco-Tougas, M., and Hermanson, J. C., "Penetration and Mixing of Fully Modulated Turbulent Jets in Crossflow," *AIAA Journal*, Vol. 37, No. 7, 1999, pp. 842–850.

[10]Roy, S., Nasr, K., Patel, P., and Abdulnour, B., "An Experimental and Numerical Study of Heat Transfer off an Inclined Surface Subject to an Impinging Airflow," *International Journal of Heat and Mass Transfer* (to be published).

[11]Yakhot, V., and Orszag, S. A., "Renormalization Group Analysis of Turbulence. I. Basic Theory," *Journal of Scientific Computing*, Vol. 1, No. 1, 1986, pp. 3–51.

[12]Brooks, A. N., and Hughes, T. J. R., "Streamline Upwind/Petrov-Galerkin Formulations for Convection Dominated Flows with Particular Emphasis on the Incompressible Navier–Stokes Equations," *Computer Methods in Applied Mechanics and Engineering*, Vol. 32, No. 1–3, 1982, pp. 199–259.

[13]Patankar, S. V., *Numerical Heat Transfer and Fluid Flow*, Hemisphere, Washington, DC, 1980, pp. 123–126.

[14]Moffat, R. J., "Describing the Uncertainties in Experimental Results," *Experimental Thermal and Fluid Science*, Vol. 1, No. 1, 1988, pp. 3–17.

Numerical Model of the Plasma Jet Generated by an Electrothermal-Chemical Igniter

Michael J. Nusca,* Michael J. McQuaid,† and William R. Anderson‡
U.S. Army Research Laboratory, Aberdeen Proving Ground, Maryland 21005-5066

Introduction

THE electrothermal-chemical (ETC) gun propulsion concept is currently being investigated by the military services. In the ETC gun, energy, which is stored either in batteries or a rotating device, is converted on demand into an electrically generated plasma (resulting from the ablation of polyethylene material in a capillary) that is injected into the chamber of a cannon or gun. This plasma energy is used to ignite the chemical propulsion charge (i.e., solid propellant) as well as to enhance gun performance by taking advantage of a number of unique plasma characteristics. For example, a low-density plasma jet can 1) efficiently ignite charges of high loading density; 2) control propellant mass generation rates[1]; 3) reduce propellant charge temperature sensitivity, that is, the variation of gun performance with changing ambient temperature[2]; and 4) shorten ignition delay, that is, the time interval between firing of the igniter and ignition of the propellant.[3] Because a plasma has a much lower density than the gases generated by a chemical igniter, it has been suggested that energy transport by convection might be as important as radiation transport in plasma-propellant interactions.[4] The plasma is at a temperature that is considerably higher than conventional chemical igniters; thus, radiation effects are nearly 100 times greater than that of chemical igniters (i.e., a T^4 effect). All of these effects can lead to useful improvements in gun performance.

A goal of ETC gun research is to elucidate the relevant physical, mechanical, and chemical mechanisms that underlie the observed ballistic effects. The first phase of the modeling effort involves a time-accurate computational fluid dynamics (CFD) code, which includes high-temperature thermodynamics, variable specific heats and transport properties (viscosity and thermal conductivity), and finite rate (nonequilibrium) chemical kinetics (the chemical mechanism is described in Ref. 5). A separate ETC capillary (i.e., igniter) model,[6] which includes a simulation of electrical currents in the ionized plasma, supplies boundary conditions for the CFD code in terms of the physical and chemical properties of the capillary efflux (plasma). Validation of the capillary model has been reported separately.[6] Validation of the CFD code, including coupled chemistry, is conducted by simulating a series of experiments wherein

Presented as Paper 2000-2675 at the AIAA 31st Plasmadynamics and Lasers Conference, Denver, CO, 19–22 June 2000; received 26 February 2001; accepted for publication 20 September 2001.

*Aerospace Engineer, Weapons and Materials Research Directorate. Associate Fellow AIAA.
†Physical Scientist, Weapons and Materials Research Directorate.
‡Research Chemist, Weapons and Materials Research Directorate.